

Citation for published version:
Gong, X, De Paola, A, Angeli, D & Strbac, G 2019, 'A Game-Theoretic Approach for Price-Based Coordination of Flexible Devices Operating in Integrated Energy-Reserve Markets', *Energy*, vol. 189, 116153, pp. 1-12. https://doi.org/10.1016/j.energy.2019.116153

10.1016/j.energy.2019.116153

Publication date: 2019

Document Version Peer reviewed version

Link to publication

Publisher Rights CC BY-NC-ND

# **University of Bath**

# **Alternative formats**

If you require this document in an alternative format, please contact: openaccess@bath.ac.uk

**General rights** 

Copyright and moral rights for the publications made accessible in the public portal are retained by the authors and/or other copyright owners and it is a condition of accessing publications that users recognise and abide by the legal requirements associated with these rights.

If you believe that this document breaches copyright please contact us providing details, and we will remove access to the work immediately and investigate your claim.

Download date: 08, Mar. 2023

# A Game-Theoretic Approach for Price-Based Coordination of Flexible Devices Operating in Integrated Energy-Reserve Markets

Xuan Gong<sup>a,\*</sup>, Antonio De Paola<sup>b</sup>, David Angeli<sup>a,c</sup>, Goran Strbac<sup>a</sup>

<sup>a</sup>Department of Electrical and Electronic Engineering, Imperial College London, UK
<sup>b</sup>Department of Electronic and Electrical Engineering, University of Bath, UK
<sup>c</sup>Department of Information Engineering, University of Florence, Italy

#### **Abstract**

This paper presents a novel distributed control strategy for large scale deployment of demand response. In the considered framework, large populations of storage devices and electric vehicles (EVs) participate to an integrated energy-reserve market. They react to prices and autonomously schedule their operation in order to optimize their own objective functions. The price signals are obtained through the resolution of an optimal power flow problem that explicitly takes into account the impact of demand response on the optimal power dispatch and reserve procurement of committed generation. Differently from previous approaches, the adopted game-theoretic framework provides rigorous theoretical guarantees of convergence and optimality of the proposed control scheme in a multi-price setup that includes ancillary services. The performance of the coordination scheme is also evaluated in simulation on the PJM 5-bus system, demonstrating its capability to flatten demand profiles and reduce the costs of generators and flexible devices.

*Keywords:* Integrated market, Demand response, Electric vehicles, Storage, Reserve service, Game theory.

<sup>\*</sup>Corresponding author

Email addresses: xuan.gong15@imperial.ac.uk (Xuan Gong), adp50@bath.ac.uk (Antonio De Paola), d.angeli@imperial.ac.uk (David Angeli), g.strbac@imperial.ac.uk (Goran Strbac)

# Nomenclature

#### **Indices and Sets**

- $m(\mathcal{M})$  Index (set) of nodes
- $l(\mathcal{L})$  Index (set) of transmission lines
- $t(\mathcal{T})$  Index (set) of time instants
- $j(\mathcal{N})$  Index (set) of flexible devices
- $\mathcal{N}^{EV}$  Set of EVs
- $\mathcal{N}^S$  Set of storage devices
- $U_i$  Set of feasible power profiles of device j

# **Parameters**

- s(l) Sending node of transmission line l
- r(l) Receiving node of transmission line l
- $X_l$  Reactance of transmission line l
- $\bar{F}_l$  Capacity of transmission line l
- $\bar{G}_m$  Capacity of the generation at node m
- $G_m$  Minimum power generation at node m
- $\Delta G_L^{max}$  Loss of the largest power unit
- $\Delta t$  Time discretization step
- $\bar{P}_i$  Maximum charging rate of EV or storage j
- $A_j$  Time availability interval of EV j
- $T_i^s$  Starting charging time of EV j
- $T_j^e$  Ending charging time of EV j

- $E_j$  Energy amount required by EV j
- $E_{j,0}$  Initial energy level of storage j
- $\underline{P}_j$  Maximum discharging rate of storage j
- $\bar{E}_j$  Energy capacity of storage j

## **Variables**

- $D_{m,t}$  Power demand at node m at time t
- $G_{m,t}$  Power generation at node m at time t
- $R_{m,t}^0$  Reserve provided by generation at node m at time t
- $R_{m,t}$  Reserve provided by flexible devices at node m at time t
- $\theta_{m,t}$  Voltage angle at node m at time t
- $F_{l,t}$  Power flow at line l at time t
- $u_i \in \mathbb{R}^T$  Power profile of device j
- $u_i^* \in \mathbb{R}^T$  Power profile of device j at equilibrium
- $u \in \mathbb{R}^{NT}$  Power profiles of the whole population of flexible devices
- $E_{j,t}$  Energy level of storage j at time t

# **Functions**

- $f_m^G(\cdot)$  Energy cost function of the generation at node m
- $f_m^R(\cdot)$  Reserve cost function of the generation at node m
- $\varphi(D,R)$  Minimized total cost of generations
- $p_{m,t}(D,R)$  Electricity price at node m at node t
- $\rho_{m,t}(D,R)$  Reserve price at node m at node t
- $r_{j,t}(\cdot)$  Reserve amount provided by device j at time t

```
\tilde{D}_{m,t}(u) Power demand at node m at time t when power schedule is u
```

 $\tilde{R}_{m,t}(u)$  Reserve provided by flexible devices at node m at time t

```
\tilde{p}_{m,t}(u) Electricity price at node m at time t
```

 $\tilde{\rho}_{m,t}(u)$  Reserve price at node m at time t

 $C(u, u_i)$  Cost of device j

 $\psi(u_i)$  Discomfort cost of EV j

#### 1. Introduction

Recent technological developments and the ongoing electrification of transportation and heating [1–3] are leading to unprecedented changes in power systems. The diffusion of domestic storage, "smart" appliances and electric vehicles (EVs) will soon ensure an increased flexibility on the demand side, which could be used to support the system and improve its reliability and efficiency [4–7]. However, in order to fully achieve these potential benefits, it is crucial to design scalable and robust control schemes that are able to coordinate large population of new devices and align the global system objectives with the local requirements of customers.

A wide array of different techniques has been proposed to tackle this issue. In particular, a substantial amount of research has investigated game-theoretic frameworks [8–14]. With this approach, the individual devices are modelled as self-interested rational agents that autonomously determine their operational schedule in response to prices, with the purpose of optimizing their own objective function. Through iterative updates of the control/price signals, these works analytically demonstrate the convergence of their proposed coordination schemes to a stable system configuration, usually characterized as a Nash equilibrium. However, these approaches utilize very simplistic pricing models (usually assuming that the price of electricity is a monotone increasing function of power demand) and they do not envision the possibility for the flexible devices to also provide ancillary services.

This active participation of demand response to system operation has been assessed with different approaches. For example, a bi-level scheme is proposed in [15] to coordinate the scheduling problem between an isolated microgrid and EV battery swapping stations in multi-stakeholder scenarios, taking into account demand response. Centralized methods for primary frequency support in microgrids are presented in [16] and reward allocation mechanisms are proposed in [17] to enable provision of ancillary services by thermostatically controlled loads. Market frameworks have also been widely investigated for the provision of frequency response [18, 19] and reserve services [20–23]. These papers consider flexible demand that actively participates to ancillary services markets. However, [18–23] do not provide any theoretic guarantee of convergence and optimality of their proposed market setup. Moreover, they generally require demand aggregators to coordinate the individual loads and translate their flexibility into financial rewards.

This paper bridges the gap between the game-theoretic schemes in [8–14] and the market approaches proposed in [18–23]. In particular, it considers large populations of flexible devices that individually participate to an integrated energy-response market. This scenario is analysed through a rigorous game-theoretic setup in order to formally demonstrate convergence of the proposed coordination scheme to an optimal configuration.

The problem is analysed through an agent-based framework: each individual device is modelled as a self-interested agent that responds to price signals and determines its operational schedule in order to optimize its own objective function. In addition to the minimization of the energy cost, the individual device will also aim to maximize the rewards received for reserve allocation. The agents are coordinated through an iterative scheme: they sequentially update their scheduled power profile in order to improve, at each step, their objective function. Using Lyapunov techniques, it is demonstrated that this iterative technique converges to a stable market configuration (characterized as an aggregative equilibrium) that is also socially optimal. Simulations are carried out on the PJM 5-bus system to assess the performance of the proposed scheme.

# 2. System Model

The considered power system is composed by a set  $\mathcal{M}=\{1,\ldots,M\}$  of nodes connected by a set  $\mathcal{L}=\{1,\ldots,L\}$  of transmission lines. The analysis is performed over a discrete time interval  $\mathcal{T}=\{1,\ldots,T\}$ , with a time discretization step  $\Delta t$ . Power demand is denoted by the vector  $D\in\mathbb{R}^{MT}$ , whose single component  $D_{m,t}$  corresponds to the total power consumption at node m at time t. With a similar notation,  $F_{l,t}$  indicates the power flow over line  $l\in\mathcal{L}$  at time  $t\in\mathcal{T}$  from the sending node  $s(l)\in\mathcal{M}$  to the receiving node  $r(l)\in\mathcal{M}$ . Generation, reserve and voltage angle vectors are denoted as  $G\in\mathbb{R}^{MT}$ ,  $R^0\in\mathbb{R}^{MT}$  and  $\theta\in\mathbb{R}^{MT}$ , respectively.

It is assumed that the power system operates under an integrated energy-reserve market. Consistently with the approach presented in [24] and [25], an optimal power flow (OPF) is solved to optimally dispatch power and procure reserve capacity, modeled as follows.

$$\varphi(D,R) = \min_{G,R^0,\theta} \sum_{m=1}^{M} \sum_{t=1}^{T} \left( f_m^G(G_{m,t}) + f_m^R(R_{m,t}^0) \right) \tag{1}$$

subject to:

$$D_{m,t} - G_{m,t} + \sum_{\{l:s(l)=m\}} F_{l,t} - \sum_{\{l:r(l)=m\}} F_{l,t} = 0 \qquad \forall m \in \mathcal{M}$$
 (2a)

$$|F_{l,t}| = \left| \frac{1}{X_l} \cdot \left[ \theta_{r(l),t} - \theta_{s(l),t} \right] \right| \le \bar{F}_l \quad \forall l \in \mathcal{L}, \quad \forall t \in \mathcal{T}$$
 (2b)

$$\underline{G}_m \le G_{m,t} \le \bar{G}_m \qquad \forall m \in \mathcal{M}, \quad \forall t \in \mathcal{T}$$
 (2c)

$$R_{m,t}^0 \le \bar{G}_m - G_{m,t} \qquad \forall m \in \mathcal{M}, \quad \forall t \in \mathcal{T}$$
 (2d)

$$\sum_{m=1}^{M} \left( R_{m,t}^{0} + R_{m,t} \right) \ge \Delta G_{L}^{max} \quad \forall t \in \mathcal{T}.$$
 (2e)

The objective function in the right-hand side of (1) corresponds to the sum (over all times t and buses m) of the generation cost  $f_m^G(G_{m,t})$  for producing  $G_{m,t}$  units of power and the cost  $f_m^R(R_{m,t}^0)$  for providing  $R_{m,t}^0$  units of reserve. The functions  $f_m^G$  and  $f_m^R$  are assumed to be strictly convex.

Regarding the constraints, (2a) corresponds to the supply-demand balance. The inequalities in (2b) ensure that the power flow  $F_{l,t}$  does not exceed the line capacity  $\bar{F}_l$ , whereas (2c) imposes that generation at bus m is always within the minimum  $G_m$  and maximum  $\bar{G}_m$  capability. The amount of reserve  $R_{m,t}^0$  that can be procured by generation at bus m at time t is constrained by (2d) and cannot exceed the extra available capacity. Finally, (2e) imposes that the total allocated reserve exceeds some minimum quantity  $\Delta G_L^{max}$ , which for example could be the largest power unit capacity. Note that, in the left-hand side of (2e), the total procured reserve is calculated as the sum over all buses of two components: the reserve  $R_{m,t}^0$  procured by the committed generation and the reserve  $R_{m,t}$  provided by flexible devices, which will be characterized in the next section.

Under this paradigm, the prices for energy and reserve provision can be defined:

$$p_{m,t}(D,R) = \frac{\partial \varphi(D,R)}{\partial D_{m,t}}$$
 (3a)

$$\rho_{m,t}(D,R) = -\frac{\partial \varphi(D,R)}{\partial R_{m,t}}.$$
(3b)

The quantity  $p_{m,t}$  represents the marginal cost of accommodating an additional unit of demand at node m at time t and it can be interpreted as the price of electricity at that bus and time instant. Similarly, the quantity  $\rho_{m,t}$  represents the marginal saving obtained if flexible devices increase by an additional unit their allocated reserve  $R_{m,t}$  at node m at time t (counterbalanced by an opposite reduction of  $R_{m,t}^0$  from generators). As a result,  $\rho_{m,t}$  can be considered the price at which the allocation of reserve by flexible devices is rewarded.

**Assumption 1.** The function  $\varphi(D,R)$  is differentiable with respect to  $D_{m,t}$  and  $R_{m,t}$  for any  $m \in \mathcal{M}$  and  $t \in \mathcal{T}$ . Its derivatives  $p_{m,t}(D,R)$  and  $\rho_{m,t}(D,R)$  in (3) are

Lipschitz continuous.

The hypothesis of global differentiability of  $\varphi$  is introduced to simplify the subsequent analysis and ensure that the prices p and  $\rho$  in (3) are always well-defined. It can be extended to the case of  $\varphi$  differentiable almost everywhere by using the double-price framework presented in [26].

## 3. Price-Responsive Flexible Devices

Flexible devices have flexibility in adjusting their power consumption, which could potentially change the system demand and provide reserve. This section proposes an agent-based modelling of flexible devices, presenting their dynamics and objectives and characterizing their overall impact on the power system.

## 3.1. Dynamics and Constraints

Consider a population  $\mathcal{N}=\{1,\ldots,N\}$  of flexible devices partitioned into two groups: the set  $\mathcal{N}^{EV}$  of EVs and the set  $\mathcal{N}^S$  of storage batteries. Each device  $j\in\mathcal{N}$  operates over the time interval  $\mathcal{T}$  according to a scheduled power profile  $u_j=[u_{j,1},\ldots,u_{j,T}]\in\mathbb{R}^T$ , where  $u_{j,t}$  denotes the power charged/discharged by device j at time t. The feasibility of  $u_j$  is now characterized for EVs and storage.

*EVs*: Each EV  $j \in \mathcal{N}^{EV}$  has rated power  $\bar{P}_j$  and requires a certain amount of energy  $E_j$  to fully charge its battery. Its charging can only occur within the interval  $\mathcal{A}_j = \{T_j^s, T_j^s + 1, \dots, T_j^e\} \subseteq \mathcal{T}$ , when the EV is plugged into the grid. Therefore, the set  $\mathcal{U}_j$  of all feasible charging profiles  $u_j$  for an EV j can be defined:

$$\mathcal{U}_j := \left\{ u_j \in \mathbb{R}^T : \sum_{t=1}^T u_{j,t} \cdot \Delta t = E_j , \ 0 \le u_{j,t} \le \bar{P}_j \cdot \mathbb{1}_{\mathcal{A}_j}(t) \quad \forall t \in \mathcal{T} \right\}$$
(4)

where  $\mathbb{1}_{A_i}(t)$  is the indicator function:

$$\mathbb{1}_{\mathcal{A}_j}(t) = \begin{cases} 1 & \text{if} \quad t \in \mathcal{A}_j \\ 0 & \text{if} \quad t \notin \mathcal{A}_j. \end{cases}$$
 (5)

The equality in (4) guarantees that the energy charged by the EV j over  $\mathcal{T}$  is equal to required amount  $E_j$ , while the inequalities indicate that the positive charging rate of the EV j cannot exceed its rated power  $\bar{P}_j$  during the availability times  $\mathcal{A}_j$  and should be zero outside  $\mathcal{A}_j$ .

**Storage Devices**: The storage device  $j \in \mathcal{N}^S$  is characterized by: its energy capacity  $\bar{E}_j$ , its maximum charging rate  $\bar{P}_j$  and discharging rate  $\underline{P}_j$ . For a certain initial energy  $E_{j,0}$  and charge/discharge profile  $u_j$ , the associated energy level  $E_{j,t}$  of storage j at time t can be expressed:

$$E_{j,t} = E_{j,0} + \sum_{x=1}^{t} u_{j,x} \cdot \Delta t.$$
 (6)

The set  $U_j$  of all feasible  $u_j$  for the storage j can therefore be defined:

$$\mathcal{U}_{j} := \left\{ u_{j} \in \mathbb{R}^{T} : \sum_{t=1}^{T} u_{j,t} = 0, \quad 0 \leq E_{j,0} + \sum_{x=1}^{t} u_{j,x} \cdot \Delta t \leq \bar{E}_{j}, \right.$$

$$\underline{P}_{j} \leq u_{j,t} \leq \bar{P}_{j} \quad \forall t \in \mathcal{T} \right\}.$$

$$(7)$$

The equality in (7) is equivalent to the cyclic constraint  $E_{j,0} = E_{j,T}$  from (6), ensuring that the initial and final storage energy levels are equal. The first and second chains of inequalities in (7) ensure that the energy level  $E_{j,t}$  and charging/discharging rate  $u_{j,t}$  remain within feasible limits.

The set  $\mathcal U$  of feasible power schedule  $u \in \mathbb R^{NT}$  for the whole population can be characterized:

$$\mathcal{U} = \mathcal{U}_1 \times \dots \times \mathcal{U}_N. \tag{8}$$

## 3.2. Reserve Service Provision

It is envisioned that EVs and storage devices can contribute to the provision of reserve by being available to reduce their power consumption. In particular, it is assumed that each device allocates the maximum feasible reserve amount, i.e. the maximum power reduction that does not violate the feasibility conditions expressed in (4) and (7). For simplicity, it is assumed that this power reduction must last for a period of time step  $\Delta t$ , which has been chosen equal to 30 minutes in the proposed case study.

**EVs**: At each time t, the reserve amount r that can be provided by the EV j corresponds to a reduction of its power consumption from its scheduled value  $u_{j,t}$  to 0.

$$r_{j,t}(u) = u_{j,t} \qquad \forall j \in \mathcal{N}^{EV}.$$
 (9)

**Storage Devices**: The reserve r that can be allocated by the storage j at time t is determined by the feasibility constraints in (7) and must fulfill the following conditions:

$$r_{i,t}(u) \le u_{i,t} - \underline{P}_i \tag{10a}$$

$$E_{j,t} - r_{j,t}(u)\Delta t = E_{j,0} + \sum_{x=1}^{t} u_{j,t}\Delta t - r_{j,t}(u)\Delta t \ge 0$$
 (10b)

Equation (10a) imposes that  $r_{j,t}(u)$  is smaller than the maximum feasible power reduction  $u_{j,t} - \underline{P}_j$  whereas (10b) ensures that a potential power reduction of  $r_{j,t}(u)$  units by storage j at time t does not violate its energy constraints. The reserve r can then be expressed as:

$$r_{j,t}(u) = \min\left(\frac{E_{j,t}}{\Delta t}, u_{j,t} - \underline{P}_j\right) \qquad \forall j \in \mathcal{N}^S.$$
 (11)

# 3.3. Aggregate Impact of Flexible Devices

It is now possible to express the parameters D and R of  $\varphi$  in (1) as functions  $\tilde{D}(u)$  and  $\tilde{R}(u)$  of the overall power schedule u of flexible devices. The total demand  $\tilde{D}_{m,t}(u)$  at bus m at time t is given by the sum of the demand  $d_{m,t}$  of inflexible devices (assumed to be known a priori) and the total power consumption of the flexible devices. Denoting by  $\mu_j \in \mathcal{M}$  the bus where the device  $j \in \mathcal{N}$  operates, it holds:

$$\tilde{D}_{m,t}(u) = d_{m,t} + \sum_{\{j: \mu_j = m\}} u_{j,t}.$$
(12)

Similarly, the total reserve  $\tilde{R}_{m,t}(u)$  has the following expression:

$$\tilde{R}_{m,t}(u) = \sum_{\{j: \mu_j = m\}} r_{j,t}(u). \tag{13}$$

Replacing the generic terms D and R in (3) with the corresponding expressions  $\tilde{D}(u)$  and  $\tilde{R}(u)$  yields:

$$\tilde{p}_{m,t}(u) := p_{m,t}(\tilde{D}(u), \tilde{R}(u)) \tag{14a}$$

$$\tilde{\rho}_{m,t}(u) := \rho_{m,t}(\tilde{D}(u), \tilde{R}(u)). \tag{14b}$$

The functions  $\tilde{p}_{m,t}(u)$  and  $\tilde{\rho}_{m,t}(u)$  correspond, respectively, to the prices of electricity and reserve as functions of the overall power schedule u by the flexible devices.

#### 4. Game-Theoretic Formulation

## 4.1. Cost of Flexible devices

On the basis of broadcast price signals, the cost C of a device j can be expressed as a function of its power profile  $u_j$  and the overall schedule u.

**EVs**: The cost C of EV j has the following expression:

$$C(u, u_j) = \sum_{t=1}^{T} [\tilde{p}_{\mu_j, t}(u) \cdot u_{j, t} - \tilde{\rho}_{\mu_j, t}(u) \cdot r_{j, t}(u)] + \psi(u_j) \quad \forall j \in \mathcal{N}^{EV}$$
 (15)

This expression includes electricity cost, reserve revenue and a discomfort cost summarized by a function  $\psi(u_j)$ . The function  $\psi$  is meant to represent the potential discomfort incurred by the EV owner if, by actually providing reserve, the vehicle battery is not fully charged by the end of the considered interval. Denoted by  $\hat{E}(u_j,t)$  the final energy mismatch if reserve is provided by the EV j at time t, the following expression is considered for  $\psi$ :

$$\psi(u_j) = \sum_{t \in \mathcal{A}_j} \xi \cdot \hat{E}(u_j, t), \tag{16}$$

where  $\xi$  is a penalty factor. The missed energy  $\hat{E}(u_j,t)$ , if positive, will correspond to the difference between the required energy  $E_j$  and the maximum energy that the EV can charge by operating at the maximum power rate  $\bar{P}_j$  after the potential reserve

service provision:

$$\hat{E}(u_j, t) = \min \left[ 0, E_j - \left( \sum_{\tau = T_j^s}^{t-1} u_{j,\tau} \Delta t + \sum_{\tau = t+1}^{T_j^e} \bar{P}_j \Delta t \right) \right].$$
 (17)

To capture the sensitivity of the cost C in (15) with respect to the power profile  $u_j$  of the single EV, the gradient  $\nabla_{u_j}C(u,u_j)=\left[\frac{\partial C(u,u_j)}{\partial u_{j,1}},\ldots,\frac{\partial C(u,u_j)}{\partial u_{j,T}}\right]$  is considered. Recalling from (9) that the provided reserve  $r_{j,t}(u)$  is equal to the power consumption  $u_{j,t}$  when  $j\in\mathcal{N}^{EV}$ , the individual components of  $\nabla_{u_j}C(u,u_j)$  have the following expression:

$$\frac{\partial C(u, u_j)}{\partial u_{j,t}} = \tilde{p}_{\mu_j, t}(u) - \tilde{\rho}_{\mu_j, t}(u) + \frac{\partial \psi(u_j)}{\partial u_{j,t}} \quad \forall j \in \mathcal{N}^{EV}.$$
 (18)

**Storage Devices**: The cost C of the storage j only considers the first two components in (15), as there is no customer discomfort associated to its final energy level:

$$C(u, u_j) = \sum_{t=1}^{T} \left[ \tilde{p}_{\mu_j, t}(u) \cdot u_{j, t} - \tilde{\rho}_{\mu_j, t}(u) \cdot r_{j, t}(u) \right] \quad \forall j \in \mathcal{N}^S.$$
 (19)

The individual components of  $\nabla_{u_i} C(u, u_j)$  have the following expression:

$$\frac{\partial C(u, u_j)}{\partial u_{j,t}} = \tilde{p}_{\mu_j, t}(u) - \sum_{s=t}^T \tilde{\rho}_{\mu_j, s}(u) \frac{\partial r_{j, s}(u)}{\partial u_{j, t}} \quad \forall j \in \mathcal{N}^S.$$
 (20)

Note that the partial derivatives  $\frac{\partial r_{j,s}(u)}{\partial u_{j,t}}$  appear in (20) only for  $s \geq t$ . This is because changes in  $u_{j,t}$  at time t only modify the energy level  $E_{j,s}$  in (6) for  $s \geq t$ . Consequently, the reserve values  $r_{j,s}(u)$  in (11) will be affected by changes in  $u_{j,t}$  only if  $s \geq t$ , implying that  $\frac{\partial r_{j,s}(u)}{\partial u_{j,t}} = 0$  when s < t.

#### 4.2. Flexible Device Operation as Competitive Game

The flexible devices can be considered as price-responsive rational players that autonomously schedule their power profiles  $u_j$  to minimize their own costs  $C(u, u_j)$ , competing for power consumption at times with lower price  $\tilde{p}(u)$  and for reserve allocation at times with higher rewarded price  $\tilde{\rho}(u)$ . The devices interact with each other

through the changes in prices introduced by their aggregate power profile. Notice in fact that variations in the individual power profiles  $u_j$  modify the overall power schedule u and change the price signals  $\tilde{p}(u)$  and  $\tilde{\rho}(u)$  in (14). For example, all devices will try to consume more power at times when  $\tilde{p}(u)$  is low. However, this will increase u and induce higher prices.

## 4.3. Aggregative Equilibrium

The power profile  $u^*$  scheduled by the flexible devices should correspond to a stable market configuration that satisfies each individual price-responsive agent. This can be characterized as an aggregative equilibrium.

**Definition 1.** Consider a feasible power schedule  $u^*$  with  $u_j^* \in \mathcal{U}_j$ ,  $\forall j$ . This corresponds to an aggregative equilibrium if the following conditions hold:

$$C(u^*, u_i^*) \le C(u^*, u_j) \qquad \forall u_j \in \mathcal{U}_j, \quad \forall j \in \mathcal{N}.$$
 (21)

Condition (21) implies that, at the equilibrium  $u^*$ , no device j can unilaterally reduce its individual cost by changing its scheduled power  $u_j^*$  into any other feasible profile  $u_j$ . This equilibrium solution proposed in this work is also fair in terms of flexibility: devices with larger availability windows will have lower costs.

To simplify the analysis, this aggregative equilibrium assumes that the strategy variation of agent j from  $u_j^*$  to some other  $u_j$  has a negligible impact on the overall schedule  $u^*$  (i.e. the first variable of the cost C) and therefore on the prices  $\tilde{p}(u^*)$  and  $\tilde{\rho}(u^*)$ . This is a reasonable approximation since the power consumption of the individual device is several order of magnitudes smaller than total power demand.

#### 5. Distributed Control Strategy

In this section we propose a distributed scheme that, by iterated price broadcasts and independent power schedule updates by the flexible devices, converges to the aggregative equilibrium in Definition 1. Convergence will be proved with Lyapunov

methods, demonstrating that a certain function V is reduced at each schedule update.

$$V(u) = \varphi(\tilde{D}(u), \tilde{R}(u)) + \sum_{j \in \mathcal{N}^{EV}} \psi(u_j).$$
 (22)

Note that V corresponds to the sum of the minimized cost  $\varphi$  and the EV discomfort  $\psi$ , thus representing a global cost index for the considered problem.

## 5.1. Elementary Power Swap

It is envisioned that the flexible devices sequentially update their power profile in response to price signals, with the objective of reducing their cost function. The fundamental power update operation of device j consists of a power swap of  $\Delta$  power units from time  $\underline{t}$  to time  $\overline{t}$ . Starting from an initial power schedule  $u \in \mathcal{U}$ , the updated global power profile  $u^+$  after the swap will have the following expression:

$$u_{i,s}^{+} = \begin{cases} u_{i,s} - \Delta & \text{if} \quad i = j, \ s = \underline{t} \\ u_{i,s} + \Delta & \text{if} \quad i = j, \ s = \overline{t} \\ u_{i,s} & \text{otherwise} \end{cases}$$
 (23)

If one denotes by  $\hat{\mathbf{e}}_{j,t}$  the vector of the standard orthogonal basis associated to the components j and t of  $\mathbb{R}^{NT}$ , the following equivalent compact expression can be provided:

$$u^{+} = u + \Delta \left( \hat{\mathbf{e}}_{j,\bar{t}} - \hat{\mathbf{e}}_{j,\underline{t}} \right) \tag{24}$$

For a certain power schedule  $u \in \mathcal{U}$ , the amount of power  $\Delta$  that can be swapped by the single device  $j \in \mathcal{N}$  is limited by the quantity  $\delta$ , defined as follows:

$$\delta(u,j,\bar{t},\underline{t}) = \min \left\{ a(u,j,\bar{t}), b(u,j,\underline{t}), c(u,j,\bar{t},\underline{t}), d(u,j,\bar{t},\underline{t}) \right\}. \tag{25}$$

Each of the four terms of the minimum function in (25) is now described in detail:

• *Maximum feasible power increase* at time  $\bar{t}$ :

$$a(u,j,\bar{t}) = \bar{P}_j - u_{j,\bar{t}} \tag{26}$$

• *Maximum feasible power decrease* at time  $\underline{t}$ :

$$b(u, j, \underline{t}) = \begin{cases} u_{j,\underline{t}} & \text{if } j \in \mathcal{N}^{EV} \\ u_{j,\underline{t}} - \underline{P}_j & \text{if } j \in \mathcal{N}^S \end{cases}$$
 (27)

The bounds a and b ensure that  $u_j^+$  in (23), i.e. the new power schedule of device j after the swap, always fulfils the power bounds in (4) and (7) when  $\Delta \leq a$  and  $\Delta \leq b$ .

• Maximum feasible power swap that fulfils energy constraints:

$$c(u, j, \bar{t}, \underline{t}) = \begin{cases} \bar{P}_{j} & \text{if } j \in \mathcal{N}^{EV} \\ \min_{\substack{t \in \{\underline{t}, \dots, \bar{t}-1\} \\ \Delta t}} \frac{E_{j,t}}{\Delta t} & \text{if } j \in \mathcal{N}^{S}, \underline{t} < \bar{t} \\ \frac{\bar{E}_{j} - \max_{t \in \{\bar{t}, \dots, \underline{t}-1\}} E_{j,t}}{\Delta t} & \text{if } j \in \mathcal{N}^{S}, \bar{t} < \underline{t} \end{cases}$$
(28)

By imposing  $\Delta \leq c$ , the energy constraint in (7) is fulfilled. In the second case in (28), it is ensured that the minimum energy level of the storage device j between  $\underline{t}$  and  $\overline{t}-1$ , which is lowered by  $c\Delta t$  as a result of the power swap, remains above zero. The third case in (28) fulfils a similar purpose when  $\overline{t} < \underline{t}$  and energy level of the storage is increased between  $\overline{t}$  and  $\underline{t}-1$ . Since no energy constraints are considered when  $j \in \mathcal{N}^{EV}$ , in the first case in (28) c corresponds to the maximum power  $\overline{P}_j$ .

Maximum cost-reducing power swap.

The last term d in (25) ensures that  $\Delta > 0$  only if the associated power swap reduces the cost of the individual device. This term can generally be defined as follows:

**Lemma 1.** For all  $j \in \mathcal{N}$ ,  $(\bar{t},\underline{t}) \in \mathcal{A}_j \times \mathcal{A}_j$ ,  $u \in \mathcal{U}$ , there exists  $d(u,j,\bar{t},\underline{t}) \geq 0$  such that, for any  $\Delta \in [0,d(u,j,\bar{t},\underline{t})]$ , the following conditions hold:

$$d(u,j,\bar{t},\underline{t}) = 0 \iff \nabla_{u_j}C(u,u_j)\left(\hat{\mathbf{e}}_{j,\bar{t}} - \hat{\mathbf{e}}_{j,t}\right) \ge 0$$
 (29a)

$$C\left(u, u_{i}^{+}\right) - C(u, u_{j}) = \nabla_{u_{j}} C(u, u_{j}) \left(\hat{\mathbf{e}}_{j, \bar{t}} - \hat{\mathbf{e}}_{j, \underline{t}}\right) \Delta \tag{29b}$$

$$\exists \alpha > 0 : V(u^{+}) - V(u) = \nabla_{u_{i}} C(u, u_{i}) \left( \hat{\mathbf{e}}_{i, \bar{t}} - \hat{\mathbf{e}}_{j, t} \right) \alpha \tag{29c}$$

PROOF OF LEMMA 1. See Appendix A.

Condition (29a) imposes that d is positive (and therefore a power swap is performed by device j between times  $\underline{t}$  and  $\overline{t}$ ) only when the gradient of C is negative. This means that also the cost variation  $C\left(u,u_j^+\right)-C(u,u_j)$  is negative, as established in (29b). Finally, (29c) ensures that the variations of C and V caused by the power swap have the same sign.

# 5.2. Coordination Algorithm

# Algorithm 1 Iterative scheme - Flexible device coordination

1. Initialization phase. Set:

$$u_j(0) \leftarrow u_j^{(0)} \in \mathcal{U}_j \quad \forall j \qquad n \leftarrow 0 \qquad conv \leftarrow 0$$

2. Power scheduling update

**WHILE** (conv = 0)

- (a)  $conv \leftarrow 1$   $n \leftarrow n+1$   $u(n) \leftarrow u(n-1)$ .
- (b) **FOR** j = 1:1:N

i. 
$$(\bar{t},\underline{t}) \leftarrow \underset{t_1,t_2}{\arg\max} \, \delta(u(n),j,t_1,t_2)$$

$$\begin{array}{l} \text{ii.} \ \ u_{j,\overline{t}}(n) \leftarrow u_{j,\overline{t}}(n) + \delta(u(n),j,\overline{t},\underline{t}) \\ u_{j,\underline{t}}(n) \leftarrow u_{j,\underline{t}}(n) - \delta(u(n),j,\overline{t},\underline{t}) \end{array}$$

iii. **IF** 
$$\delta(u(n), j, \bar{t}, \underline{t}) > 0 : conv \leftarrow 0$$
.

#### **END FOR**

## **END WHILE**

3. **Final results**. The power schedule at the last iteration corresponds to the aggregative equilibrium:

$$u^* \leftarrow u(n)$$
.

The proposed coordination strategy is described in Algorithm 1, which includes three main phases. In the **Initialization phase**, the power schedule of the devices is initialized to some arbitrary  $u^{(0)} \in \mathcal{U}$ . Two additional variables are also initialized: nkeeps track of the number of iterations in the algorithm, whereas the flag variable conv indicates whether an equilibrium has been reached and the update iterations can thus be terminated. In the Power scheduling update, the execution of a FOR cycle corresponds that all devices from j = 1 to j = N have updated their power schedule once, and the iteration number n will increase by one accordingly. The schedule updating of a single device j is performed as follows. First, in step 2.b.i) the device j selects a pair of time instants  $(\bar{t},\underline{t})$  that maximize the non-negative function  $\delta$ . The maximization of  $\delta$ , associated to a cost-reducing power swap, is determined based on the current overall schedule u(n) and the consequent prices  $\tilde{p}(u(n))$  and  $\tilde{\rho}(u(n))$ . Then the power amount  $\delta$  is swapped from time t to  $\bar{t}$  in step 2.b.ii), where the power schedule  $u_i(n)$  (as well as u(n) is updated. Note that the next device j+1 will update its schedule based on the updated u(n). Finally, in step 2.b.iii) conv is set to 0 if the current  $\delta$  is greater than zero, to signal that the devices are still improving their strategy and convergence has not been reached yet. When the non-negative  $\delta$  maximized in step 2.b.i) is equal to zero for all devices, conv remains equal to one throughout the whole FOR cycle and the **Final results** phase is reached, returning the desired equilibrium solution  $u^*$ .

The convergence and optimality of the proposed coordination scheme are now formally demonstrated.

**Theorem 1.** Under Assumption 1, for any population N of flexible devices operating in the power system, Algorithm 1 asymptotically converges to an aggregative equilibrium  $u^*$ .

PROOF OF THEOREM 1. See Appendix B.

**Theorem 2.** The final aggregative equilibrium  $u^*$  is a global minimizer of the function V:

$$V(u^*) \le V(u) \qquad \forall u \in \mathcal{U}.$$
 (30)

PROOF OF THEOREM 2. See Appendix C.

## 6. Performance and advantages of proposed approach

This section highlights some fundamental features of the coordination algorithm.

#### 6.1. Agent-based modelling

The proposed approach utilizes a multi-agent framework where each device independently schedules its operational strategy. This framework does not require any aggregator, i.e. an intermediate entity coordinating the flexible loads installed in multiple private households, which exhibits some potential advantages:

- Economic optimality for single devices: the proposed approach ensures cost
  minimization for each individual device. This might not be the case when aggregators are considered, since they will generally optimize only the overall operation of the devices' population.
- Maximized social welfare: as demonstrated in Theorem 2, the proposed coordination strategy is able to maximize the function V in (22), which can be interpreted as the social welfare of the system. This optimality property might not be satisfied when aggregators are considered, especially if these are self-interested entities aiming at maximizing their own profit.
- Full control of the appliances: with the approach, customers preserve full control of their devices, whose operation is not determined by external entities.

## 6.2. Distributed approach and scalability

Through the distributed framework where each device operates independently in response to price signals, the proposed approach is able to break down the complex task of coordinating large number of devices into smaller sub-problems. This avoids the computational issues of centralized approaches, which include a large number of decision variables. Although with the proposed algorithm, the time required to calculate the equilibrium solution is fundamentally linear with respect to the number  $|\mathcal{N}|$  of controlled devices, faster convergence and improved scalability can be obtained with some adjustments to the algorithm. For example:

- Simultaneous power updates by multiple devices: instead of updating and broadcasting a new price signals to a single device at each strategy update, a subset of devices can use the same price signal and modify their power profiles at once. This would reduce the number of required iterations and further enhance the scalability of the proposed method. Numerical convergence of this alternative method has been verified in simulation.
- One-shot strategy: the central entity internally emulates the proposed coordination algorithm and then performs a one-shot broadcast of the final price signal, in order to directly induce the associated equilibrium solution. This scheme, initially presented in [11] for the simpler case of smart appliances not providing ancillary services, assumes that the central coordinator would possess some general knowledge of the devices' population, based for example on estimations or on historical data.

## 7. Simulations

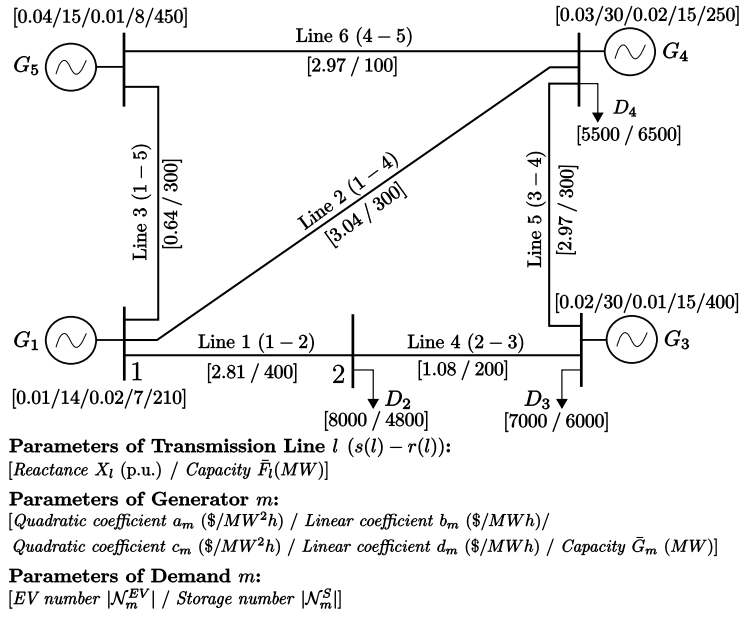


Figure 1: The PJM 5-bus system.

#### 7.1. System Model and Parameters

The coordination algorithm is tested on the PJM 5-bus system [27] in Fig. 1. A time interval of  $T=24\,\mathrm{h}$  is considered, with time discretization  $\Delta t=0.5\,\mathrm{h}$ . The generation and reserve cost functions are assumed to be quadratic, i.e.  $f_m^G(x)=\frac{1}{2}a_mx^2+b_mx$  and  $f_m^R(x)=\frac{1}{2}c_mx^2+d_mx$ . Relevant generation and transmission parameters are presented in Fig. 1. To fulfill the reserve requirement (2d), the total allocated reserve must be not less than  $\Delta G_L^{max}=\bar{G}_5=450$  MW. Inflexible demand  $d_m$  at buses m=2,3,4 has been derived from historical data [28]. It is envisioned that a population of EVs  $\mathcal{N}_m^{EV}$  and storage batteries  $\mathcal{N}_m^S$  operate at buses m=2,3,4, with  $\mathcal{N}^{EV}=\mathcal{N}_2^{EV}\cup\mathcal{N}_3^{EV}\cup\mathcal{N}_4^{EV}$  and  $\mathcal{N}^S=\mathcal{N}_2^S\cup\mathcal{N}_3^S\cup\mathcal{N}_4^S$ . A description of the two types of devices is provided below:

 $\emph{EVs}$ : The required energy amount  $E_j$  for the EV j at bus m is determined according to a Gaussian distribution with mean value  $\beta_m^E$  and a standard deviation  $\omega_m^E$ . Additionally, the rated power  $\bar{P}_j$  is set to the same value  $\bar{P}_j = 11$  kW for all  $j \in \mathcal{N}^{EV}$ . Relevant parameters are listed below:

$$\beta_2^E=\beta_3^E=\beta_4^E=30~{\rm kWh}$$
 
$$\omega_2^E=1.0~{\rm kWh}~~\omega_3^E=1.5~{\rm kWh}~~\omega_4^E=1.5~{\rm kWh}.$$

It is assumed that each EV j at node m must complete its charging within a continuous time interval  $[t_j,t_j+d_j]$ . The start time  $t_j$  and the duration  $d_j$  also follow Gaussian distributions, with mean  $\beta_m^t$  and  $\beta_m^d$  and standard deviations  $\omega_m^t$  and  $\omega_m^d$ , respectively:

$$\begin{split} \beta_2^t &= 20\text{:}30 \text{ h} & \qquad \omega_2^t = 1.5 \text{ h} & \qquad \beta_2^d = 10 \text{ h} & \qquad \omega_2^d = 1.0 \text{ h} \\ \beta_3^t &= 21\text{:}30 \text{ h} & \qquad \omega_3^t = 1.5 \text{ h} & \qquad \beta_3^d = 11 \text{ h} & \qquad \omega_3^d = 2.0 \text{ h} \\ \beta_4^t &= 21\text{:}00 \text{ h} & \qquad \omega_4^t = 1.0 \text{ h} & \qquad \beta_4^d = 11 \text{ h} & \qquad \omega_4^d = 1.5 \text{ h} \end{split}$$

Accordingly, the availability time interval  $A_j$  of EV j can be expressed in the discretized time horizon as:

$$\mathcal{A}_{j} = \{T_{i}^{s}, T_{i}^{s} + 1, \dots, T_{i}^{e}\} = \{t \in \mathcal{T} : t_{j} \leq t \cdot \Delta t \leq t_{j} + d_{j}\}.$$

**Storage Devices**: An homogeneous population of storage batteries is considered, with the following parameters:

$$\bar{P}_j = -\underline{P}_j = 2.5 \text{ kW}$$
  $\bar{E}_j = 25 \text{ kWh}$   $\forall j \in \mathcal{N}^S$ .

The total installed storage capacity is equal to  $\bar{E}_j \cdot |\mathcal{N}^S| = 432.5$  MWh. The initial energy levels  $E_{j,0}$  are determined stochastically, according to a uniform distribution with support  $[0, \bar{E}_j]$ .

# 7.2. Algorithm Implementation and Results

In the **Initialization phase** of Algorithm 1, the initial power schedule  $u_j^{(0)} \in \mathcal{U}_j$  is chosen as a constant power profile over the availability interval  $\mathcal{A}_j$  when  $j \in \mathcal{N}^{EV}$  and is identically equal to zero when  $j \in \mathcal{N}^S$ . The **WHILE** cycle in the **Power scheduling update** phase is iterated n=15 times. Simulations have required about 90 minutes on a standard PC machine with a 4-core 2.40 GHz Intel(R) Xeon(R) E5620 processor and 12 GB of RAM. The final results are compared to a No-Flexibility scenario (denoted as **NF**), where the devices do not react to price signals, do not provide reserve and simply apply the initial power schedule  $u^{(0)}$ .

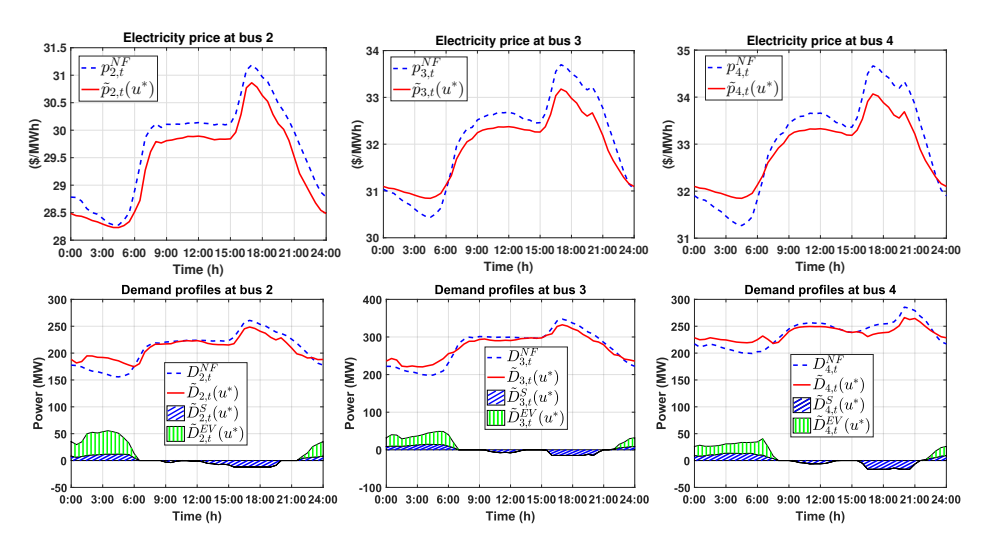


Figure 2: Electricity prices (top) and demand profiles (bottom) at each bus, when the **NF** scenario (blue dashed lines) and the proposed solution (red lines) are considered. For the latter, the shaded areas represent the power contribution of storage and EVs.

Fig. 2 compares the electricity price profiles and the power demand obtained with the proposed algorithm and in the **NF** scenario. It can be seen that prices are different at each node and are generally flattened by the coordination algorithm. It is interesting to note that, at bus 2, the price  $\tilde{p}_{2,t}$  is lower than  $p_{2,t}^{NF}$  also during the first hours of the

day, when the demand  $\tilde{D}_{2,t}$  is higher than  $D_{2,t}^{NF}$ . This is due to the interplay between demand D and allocated reserve R in the price expressions (3) and the fact that, in the NF scenario, EVs and storage do not provide any reserve, thus indirectly impacting also electricity prices. A similar flattening trend can be seen in the demand profiles: a substantial peak-shaving/valley-filling is introduced by the algorithm. From the disaggregation of flexible devices  $\tilde{D}(u^*)$  in storage component  $\tilde{D}^S(u^*)$  and EV component  $\tilde{D}^{EV}(u^*)$ , it can be seen that the EVs schedule their charge during night-time, when electricity prices are lower. Similarly, the storage devices perform energy arbitrage by charging during night time and discharging at peak times.

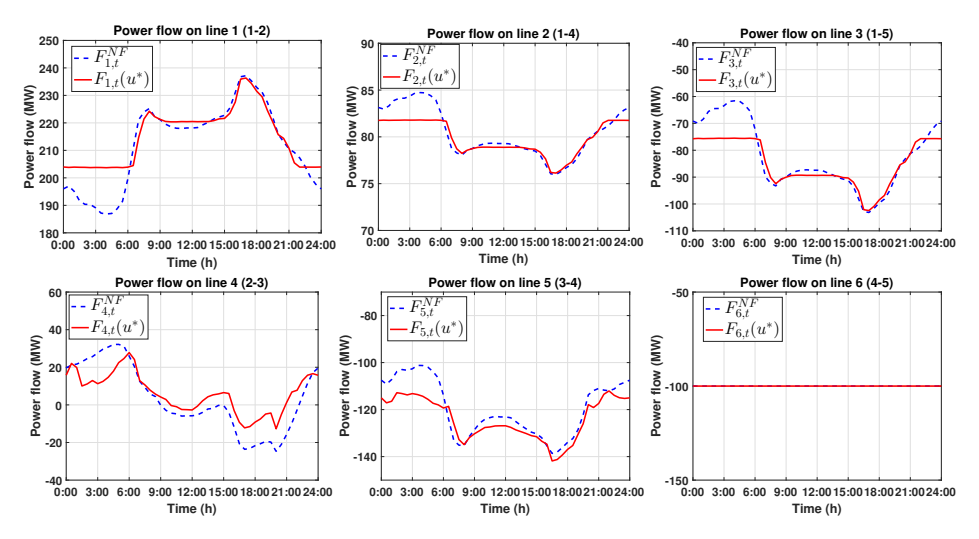


Figure 3: Power flows on transmission lines.

The power flows  $F(u^*)$  and  $F^{NF}$  in the two scenarios are compared in Fig. 3, showing that the algorithm reduces the variation over time of the power flow. The negative values on some lines indicate that power is flowing in the direction opposite to the conventional one (e.g., power is flowing from node 5 to node 1 on line 3). Note that line 6 remains congested and operates at its capacity 100 MW over 24 h. This leads to different locational marginal prices throughout the network, as shown in Fig. 2.

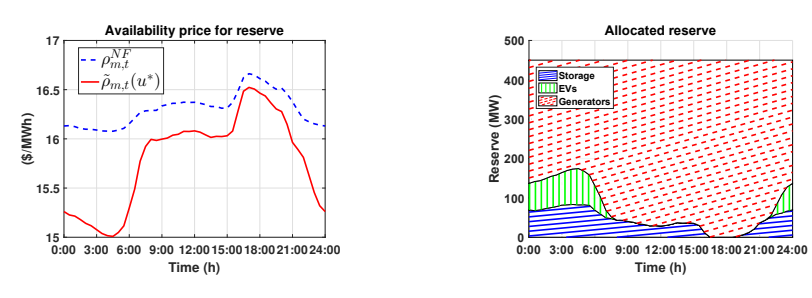


Figure 4: Reserve price (left) and allocated reserve (right).

Fig. 4 compares the prices for reserve provision at the equilibrium and in the NF scenario and shows the disaggregation of allocated reserve from different sources through the algorithm. Note that the reserve price  $\tilde{\rho}_{m,t}(u^*)$  obtained with the proposed strategy is always lower than the price  $\rho_{m,t}^{NF}$  in the NF scenario. This is to be expected since, by providing reserve, the flexible devices reduce the marginal price of additional units of reserve. In the right part of Fig. 4, it can be seen how the EVs mostly provide reserve during the early hours of the day (when they are charging and therefore are available to reduce their power consumption). Conversely, the contribution of storage covers almost the whole day, with the exception of the interval between t=16:00 h and t=21:00 h, when the batteries are mostly discharging.

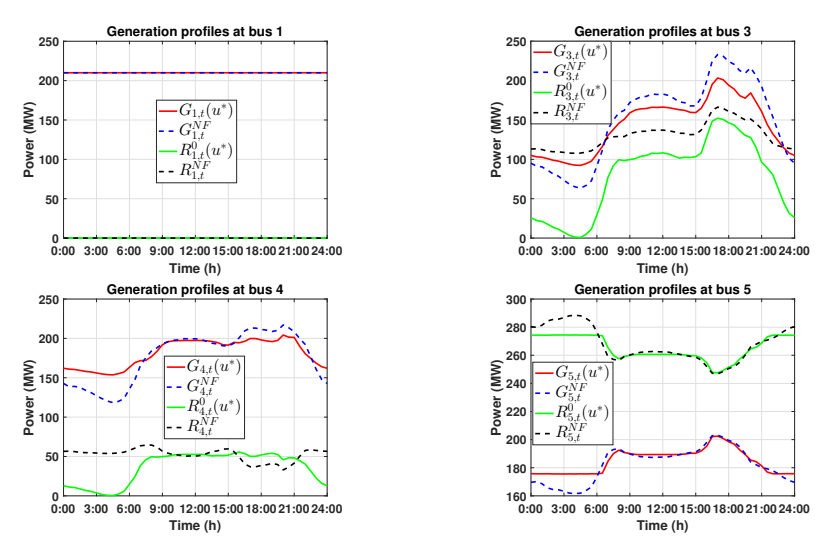
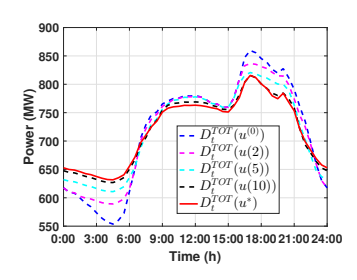


Figure 5: Power production and allocated reserve at each bus.

The power production and allocated reserve of the generators are shown in Fig. 5. Note that the capacity of the generator at bus 1 is fully allocated to power production (no reserve is provided). For the generators at the other buses, when Algorithm 1 is applied there is a reduction of reserve and an increase of power production during the early hours of the day to accommodate the higher demand from flexible devices.



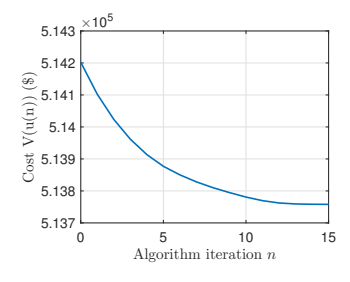


Figure 6: Comparison of total demand profiles (left) and global cost V(u(n)) as a function of the algorithm iteration n (right).

The aggregate demand profiles  $D_t^{TOT}(u(n)) = \sum_{m=1}^M \tilde{D}_{m,t}(u(n))$  – at different iterations n – are provided on the left of Fig. 6, showing that how the sequential power swaps from the flexible devices gradually flatten the demand profile. The right part of Fig. 6 shows the values of V(u(n)) in (22) at each iteration n. Note that V(u(n)) is reduced at each step and reaches a minimum at n=15, as established in Theorem 2.

Table 1: Daily costs sustained by generators and single EV/storage devices.

Scenario	No Flexibility (NF)			Proposed algorithm		
Cost (\$)	Total	Energy	Reserve	Total	Energy	Reserve
Generation	$5.402 \cdot 10^5$	$4.118 \cdot 10^5$	$1.284 \cdot 10^5$	$5.133 \cdot 10^5$	$4.107 \cdot 10^5$	$1.026 \cdot 10^5$
EVs	0.92	0.92	0	0.47	0.91	-0.46
Storage	0	0	0	-0.96	-0.03	-0.93

A comparison of the daily costs sustained by generation and individual flexible devices in the two scenarios is presented in Table 1. From a generation perspective, the algorithm reduces total costs by approximatively 5%, with particularly lower costs for reserve allocation. It should be emphasized that the comparison does not consider the payments made in the proposed algorithm to EVs and storage for reserve allocation, which in the present case amount to 25, 519 \$. From an EV perspective, total costs are halved with the algorithm: this is the result of substantial revenues for reserve alloca-

tion and a marginal reduction in the electricity costs. Note that the total cost for single EV is not equal to the sum of the energy and reserve components, as EVs also incur in an average discomfort cost of 0.02 \$, as defined in (16). Storage devices are assumed not to operate and have zero costs in the **NF** scenario. When the algorithm is applied, as in the EV case, storage will obtain most of its revenues for reserve allocation.

#### 8. Conclusions

This paper presents a novel game-theoretic scheme for coordination of price responsive flexible devices operating in an integrated energy-reserve market. The proposed algorithm ensures the convergence to a stable market configuration which is also globally optimal. The algorithm is tested in simulation on the PJM 5-bus system, demonstrating its capability to flatten demand profiles at each node while reducing costs for generators and flexible devices.

## Acknowledgments

The authors would like to acknowledge support from the Leverhulme Trust, Grant ECF-2016-394.

## Appendix A. Proof of Lemma 1

Note that (29a) can be verified by construction and the lemma holds if there exists  $\bar{\Delta} > 0$ , different in general for (29b) and (29c), such that these conditions are satisfied when  $\nabla_{u_j} C(u, u_j)$  ( $\hat{\mathbf{e}}_{j,\bar{t}} - \hat{\mathbf{e}}_{j,t}$ ) < 0 and  $\Delta \in [0, \bar{\Delta}]$ .

Proof of (29b): When  $j \in \mathcal{N}^{EV}$ , the only term in (18) which depends on  $u_j$  is the derivative of the discomfort cost  $\partial \psi(u_j)/\partial u_{j,t}$ . Since  $\hat{E}(u_j,t)$  in (17) is piecewise linear, the same holds for  $\psi(u_j)$  in (16). This means that  $\partial \psi(u_j)/\partial u_{j,t}$  and the cost derivative  $\partial C(u,u_j)/\partial u_{j,t}$  are piecewise constant  $\forall t \in \mathcal{T}$ . As a result, there always exists  $\bar{\Delta} > 0$  such that:

$$\frac{\partial C(u, u_j + \hat{\mathbf{e}}_{j,\bar{t}}s - \hat{\mathbf{e}}_{j,\underline{t}}s)}{\partial u_{j,\bar{t}}} = \frac{\partial C(u, u_j)}{\partial u_{j,\bar{t}}} \qquad \forall s \in [0, \bar{\Delta}] \tag{A.1a}$$

$$\frac{\partial C(u, u_j + \hat{\mathbf{e}}_{j, \bar{t}} s - \hat{\mathbf{e}}_{j, \underline{t}} s)}{\partial u_{j, \underline{t}}} = \frac{\partial C(u, u_j)}{\partial u_{j, \underline{t}}} \qquad \forall s \in [0, \bar{\Delta}]. \tag{A.1b}$$

To take into account the possibility of  $u_j$  being a discontinuity point (where the cost derivative switches between two constant values), it is assumed that the left and right derivative are considered in (A.1a) and (A.1b), respectively. Given  $\bar{\Delta}$  and the associated modified strategy  $u_j^+ = u_j + \left(\hat{\mathbf{e}}_{j,\bar{t}} - \hat{\mathbf{e}}_{j,\underline{t}}\right)\bar{\Delta}$ , it holds:

$$C(u, u_j^+) - C(u, u_j) = \int_0^{\bar{\Delta}} \nabla_{u_j} C(u, u_j + \hat{\mathbf{e}}_{j,\bar{t}} s - \hat{\mathbf{e}}_{j,\underline{t}} s) \left( \hat{\mathbf{e}}_{j,\bar{t}} - \hat{\mathbf{e}}_{j,\underline{t}} \right) ds$$

$$= \int_0^{\bar{\Delta}} \nabla_{u_j} C(u, u_j) \left( \hat{\mathbf{e}}_{j,\bar{t}} - \hat{\mathbf{e}}_{j,\underline{t}} \right) ds = \nabla_{u_j} C(u, u_j) \left( \hat{\mathbf{e}}_{j,\bar{t}} - \hat{\mathbf{e}}_{j,\underline{t}} \right) \bar{\Delta}. \quad (A.2)$$

Equation (A.2) also holds in the case  $j \in \mathcal{N}^S$  by considering r instead of  $\psi$  in the proof above.

 $Proof \ of \ (29c)$ : Consider the following parametrized expression W for the variation of the function V:

$$W(\Delta) = V(u + (\hat{\mathbf{e}}_{j,\bar{t}} - \hat{\mathbf{e}}_{j,\underline{t}}) \Delta) - V(u) = V(u^+) - V(u)$$
$$= \varphi(\tilde{D}(u^+), \tilde{R}(u^+)) - \varphi(\tilde{D}(u), \tilde{R}(u)) + \psi(u_j^+) - \psi(u_j) \quad (A.3)$$

When  $j \in \mathcal{N}^{EV}$ , we have  $\partial D_{\mu_j,t}(u)/\partial u_{j,t} = \partial R_{\mu_j,t}(u)/\partial u_{j,t} = 1$ . Therefore, if we consider  $\tilde{u}(s) = u + \left(\hat{\mathbf{e}}_{j,\bar{t}} - \hat{\mathbf{e}}_{j,t}\right)s$ , it holds:

$$W(\Delta) = \int_{0}^{\Delta} \frac{\partial \varphi(\tilde{D}(\tilde{u}(s)), \tilde{R}(\tilde{u}(s)))}{\partial D_{\mu_{j}, \bar{t}}} + \frac{\partial \varphi(\tilde{D}(\tilde{u}(s)), \tilde{R}(\tilde{u}(s)))}{\partial R_{\mu_{j}, \bar{t}}} - \frac{\partial \varphi(\tilde{D}(\tilde{u}(s)), \tilde{R}(\tilde{u}(s)))}{\partial D_{\mu_{j}, \underline{t}}} - \frac{\partial \varphi(\tilde{D}(\tilde{u}(s)), \tilde{R}(\tilde{u}(s)), \tilde{R}(\tilde{u}(s)))}{\partial R_{\mu_{j}, \underline{t}}} + \frac{\partial \psi(\tilde{u}_{j}(s))}{\partial u_{j, \bar{t}}} - \frac{\partial \psi(\tilde{u}_{j}(s))}{\partial u_{j, \underline{t}}} \, ds. \quad (A.4)$$

Recalling the price equations (3) and (14) and expression (19) for the cost derivative,

the quantity  $\dot{W}(\Delta) = dW(\Delta)/d\Delta$  evaluated at  $\Delta = 0$  is equal to:

$$\begin{split} \dot{W}(0) &= \left( \tilde{p}_{\mu_{j},\bar{t}}(u) - \tilde{\rho}_{\mu_{j},\bar{t}}(u) + \frac{\partial \psi(\tilde{u}_{j}(s))}{u_{j,\bar{t}}} \right) \\ &- \left( \tilde{p}_{\mu_{j},\underline{t}}(u) - \tilde{\rho}_{\mu_{j},\underline{t}}(u) + \frac{\partial \psi(\tilde{u}_{j}(s))}{u_{j,\underline{t}}} \right) = \nabla_{u_{j}} C(u,u_{j}) \left( \hat{\mathbf{e}}_{j,\bar{t}} - \hat{\mathbf{e}}_{j,\underline{t}} \right). \end{split} \tag{A.5}$$

As initially established in this proof, we are considering  $\nabla_{u_j}C(u,u_j)$   $(\hat{\mathbf{e}}_{j,\bar{t}}-\hat{\mathbf{e}}_{j,\underline{t}})<0$  and therefore we have W(0)=0 and  $\dot{W}(0)<0$ . For continuity of W and  $\dot{W}$  (ensured by Assumption 1), there exists a finite  $\bar{\Delta}$  such that  $W(\Delta)<0$  for all  $\Delta\in(0,\bar{\Delta}]$ , thus concluding the proof. Same arguments can be used to demonstrate the lemma statement when  $j\in\mathcal{N}^S$ , recalling that in this case  $\partial D_{\mu_j,t}(u)/\partial u_{j,t}=1$  and  $\partial R_{\mu_j,t}(u)/\partial u_{j,t}=\partial r_{j,t}(u)/\partial u_{j,t}$ .

#### Appendix B. Proof of Theorem 1

Proof of convergence: It is initially demonstrated that Algorithm 1 converges asymptotically to some final power schedule  $u^*$ . To this end, the following preliminary result is proved:

$$V(u(n)) < V(u(n-1)) \qquad \forall n > 0. \tag{B.1}$$

This is trivial to check when  $\delta=0$ , as in this case we have u(n)=u(n-1). When  $\delta>0$ , it is sufficient to note that  $\nabla_{u_j}C(u,u_j)\left(\hat{\mathbf{e}}_{j,\bar{t}}-\hat{\mathbf{e}}_{j,\underline{t}}\right)<0$  from (29a) and therefore, from (29b)-(29c), we have:

$$V(u(n)) - V(u(n-1)) = V(u^{+}) - V(u) < 0.$$
(B.2)

Since V is a bounded quantity, it follows from (B.1) that V(u(n)) converges to some minimum value. At such minimum the **IF** condition in step 2.b.iii) is never verified, otherwise V would be further reduced. Hence the variable conv (set to 1 in step 2.a) does not change value throughout the **FOR** cycle and it ensures that step 3) and the final power schedule  $u^*$  is reached.

*Proof of equilibrium*: To verify that the final result  $u^*$  of Algorithm 1 corresponds to the aggregative equilibrium of Definition 1, an alternative formulation is considered

for the feasible  $u_j \in \mathcal{U}_j$  of device j. In particular, each  $u_j$  can be characterized as the sum of the candidate equilibrium solution  $u^*$  and a finite number M of elementary power swaps  $\delta^{(m)}$ :

$$u_j = u_j^* + \sum_{m=1}^M \delta^{(m)}.$$
 (B.3)

Each  $\delta^{(m)}$  corresponds to swapping  $\Delta_m$  units of power from time  $\underline{t}_m$  to time  $\overline{t}_m$  and it can be expressed:

$$\delta^{(m)} = \Delta_m \left( \hat{\mathbf{e}}_{\bar{t}_m} - \hat{\mathbf{e}}_{t_m} \right). \tag{B.4}$$

The terms  $\delta^{(1)}, \dots, \delta^{(M)}$  can always be selected in order to fulfil the following feasibility conditions [29]:

$$u_j^{(m)} = u_j^* + \sum_{i=1}^m \delta^{(i)} \in \mathcal{U}_j \qquad \forall m \in \{1, \dots, M\}$$
 (B.5a)

$$\tilde{u}_{i}^{(m)} = u_{i}^{*} + \delta^{(m)} \in \mathcal{U}_{i} \qquad \forall m \in \{1, \dots, M\}.$$
 (B.5b)

Furthermore, the following condition is assumed:

$$\nabla_{u_i} C\left(u^*, u_i^* + \epsilon\left(\hat{\mathbf{e}}_{j,\bar{t}} - \hat{\mathbf{e}}_{j,\underline{t}}\right)\right) = \nabla_{u_i} C(u^*, u_i^*) \quad \forall \epsilon \in [0, \Delta_m].$$
 (B.6)

This does not introduce any loss of generality since  $\nabla_{u_j}C$  is piecewise continuous: any  $\delta^{(m)}$  with associated  $\Delta_m$  not fulfilling (B.6) can be split into multiple smaller swaps such that (B.5) and (B.6) hold.

The equilibrium result is now demonstrated by contradiction. In particular, it is assumed that  $u^*$  is not an aggregative equilibrium and there exists some  $u_j \in \mathcal{U}_j$  such that  $C(u^*, u_j) < C(u^*, u_j^*)$ . From (B.5), if this were the case, there would exist  $m \in \{1, \ldots, M\}$  such that:

$$C(u^*, u_j^* + \delta^{(m)}) < C(u^*, u_j^*).$$
 (B.7)

From the feasibility result in (B.5b) for  $u_j^* + \delta^{(m)}$ , we have:

$$a(u^*, j, \bar{t}_m) > 0 \quad b(u^*, j, \underline{t}_m) > 0 \quad c(u^*, j, \bar{t}_m, \underline{t}_m) > 0.$$
 (B.8)

From (B.7) and (B.6), it follows that  $C(u, u_j) \left( \hat{\mathbf{e}}_{j,\bar{t}} - \hat{\mathbf{e}}_{j,\underline{t}} \right) < 0$ . As a result of (29a), it holds:

$$d(u^*, j, \bar{t}_m, \underline{t}_m) > 0. (B.9)$$

We can conclude from (B.8) and (B.9) that  $\delta(u^*,j,\bar{t}_m,\underline{t}_m)$  in (25) is also positive. This is not possible, since  $u^*=u(n)$  represents the final result in step 3 of Algorithm 1, which is only reached when the variable conv remains equal to one through in step 2 and therefore  $\delta(u^*,j,\bar{t}_m,\underline{t}_m)\leq 0$ . It follows that (B.7) cannot hold, thus concluding the proof by contradiction.

# Appendix C. Proof of Theorem 2

Given the strict convexity of  $f_m^G$  and  $f_m^R$  and the linearity of all the constraints in (2), it follows that  $\varphi(D,R)$  is strictly convex. Therefore, (30) holds if the following sufficient condition is satisfied for all  $u \in \mathcal{U}$ :

$$\sum_{m=1}^{M} \nabla_{D_m} \varphi(\tilde{D}(u^*), \tilde{R}(u^*)) \left[ \tilde{D}_m(u) - \tilde{D}_m(u^*) \right]$$

$$+ \sum_{m=1}^{M} \nabla_{R_m} \varphi(\tilde{D}(u^*), \tilde{R}(u^*)) \left[ \tilde{R}_m(u) - \tilde{R}_m(u^*) \right]$$

$$+ \sum_{j \in \mathcal{N}^{EV}} \nabla_{u_j} \psi(u_j^*) (u_j - u_j^*) \ge 0 \quad (C.1)$$

Recalling (12) and (13), this corresponds to:

$$\sum_{m=1}^{M} \left[ \nabla_{D_{m}} \varphi(\tilde{D}(u^{*}), \tilde{R}(u^{*})) \sum_{\{j: \mu_{j} = m\}} \left( u_{j} - u_{j}^{*} \right) \right] \\
+ \sum_{m=1}^{M} \left[ \nabla_{R_{m}} \varphi(\tilde{D}(u^{*}), \tilde{R}(u^{*})) \sum_{\{j: \mu_{j} = m\}} \left( r_{j}(u) - r_{j}(u^{*}) \right) \right] \\
+ \sum_{j \in \mathcal{N}^{EV}} \nabla_{u_{j}} \psi(u_{j}^{*}) (u_{j} - u_{j}^{*}) \ge 0. \quad (C.2)$$

A slightly stronger condition is considered over all  $j \in \mathcal{N}$  and  $u_j \in \mathcal{U}_j$ . In the case  $j \in \mathcal{N}^{EV}$  and  $\mu_j = m$ , this corresponds to:

$$\nabla_{D_m} \varphi(\tilde{D}(u^*), \tilde{R}(u^*))(u_j - u_j^*)$$

$$+ \nabla_{R_m} \varphi(\tilde{D}(u^*), \tilde{R}(u^*))(r_j(u) - r_j(u^*)) + \nabla_{u_j} \psi(u_j^*)(u_j - u_j^*) \ge 0 \quad (C.3)$$

Since  $\nabla_{D_m}\varphi$  and  $\nabla_{R_m}\varphi$  correspond respectively to the vectors of prices  $\tilde{p}_m$  and  $\tilde{\rho}_m$ , this is equivalent to  $\nabla_{u_j}C(u^*,u_j)(u_j-u_j^*)\geq 0$ , which is always verified since  $u_j^*$  is an aggregative equilibrium according to Definition 1, thus concluding the proof.

## References

- J. Palencia, T. Sakamaki, M. Araki, S. Shiga, Impact of powertrain electrification, vehicle size reduction and lightweight materials substitution on energy use, CO2 emissions and cost of a passenger light-duty vehicle fleet, Energy 93 (2015) 1489–1504.
- [2] X. Gong, C. Xie, Y. Zou, S. Quan, B. Piotr, D. Shen, Performance and stability of supercapacitor modules based on porous carbon electrodes in hybrid powertrain, Journal of Wuhan University of Technology-Mater. Sci. Ed. 29 (6) (2014) 1141–1146.
- [3] D. Quiggin, R. Buswell, The implications of heat electrification on national electrical supply-demand balance under published 2050 energy scenarios, Energy 98 (2016) 253–270.
- [4] A. Ipakchi, F. Albuyeh, Grid of the future, IEEE Power and Energy Magazine 7 (2) (2009) 52–62. doi:10.1109/MPE.2008.931384.
- [5] R. Walawalkar, S. Fernands, N. Thakur, K. R. Chevva, Evolution and current status of demand response (DR) in electricity markets: Insights from PJM and NYISO, Energy 35 (4) (2010) 1553–1560.

- [6] P. Cappers, C. Goldman, D. Kathan, Demand response in us electricity markets: Empirical evidence, Energy 35 (4) (2010) 1526–1535.
- [7] J. Aghaei, M. I. Alizadeh, P. Siano, A. Heidari, Contribution of emergency demand response programs in power system reliability, Energy 103 (2016) 688–696.
- [8] A. Mohsenian-Rad, V. Wong, J. Jatskevich, R. Schober, A. Leon-Garcia, Autonomous demand-side management based on game-theoretic energy consumption scheduling for the future smart grid, IEEE Transactions on Smart Grid 1 (3) (2010) 320–331.
- [9] L. Gan, U. Topcu, S. H. Low, Optimal decentralized protocol for electric vehicle charging, IEEE Transactions on Power Systems 28 (2) (2013) 940–951.
- [10] Z. Ma, D. Callaway, I. Hiskens, Decentralized charging control of large populations of plug-in electric vehicles, IEEE Transactions on Control Systems Technology 21 (1) (2013) 67–78.
- [11] A. De Paola, D. Angeli, G. Strbac, Price-based schemes for distributed coordination of flexible demand in the electricity market, IEEE Transactions on Smart Grid 8 (6) (2017) 3104–3116.
- [12] B. G. Kim, S. Ren, M. V. D. Schaar, J. W. Lee, Bidirectional energy trading and residential load scheduling with electric vehicles in the smart grid, IEEE Journal on Selected Areas in Communications 31 (7) (2013) 1219–1234.
- [13] H. Chen, Y. Li, R. Louie, B. Vucetic, Autonomous demand side management based on energy consumption scheduling and instantaneous load billing: An aggregative game approach, IEEE Transactions on Smart Grid 5 (4) (2014) 1744–1754.
- [14] Z. Ma, S. Zou, L. Ran, X. Shi, I. Hiskens, Efficient decentralized coordination of large-scale plug-in electric vehicle charging, Automatica 69 (2016) 35–47.
- [15] Y. Li, Z. Yang, G. Li, Y. Mu, D. Zhao, C. Chen, B. Shen, Optimal scheduling of isolated microgrid with an electric vehicle battery swapping station in multi-stakeholder scenarios: A bi-level programming approach via real-time pricing, Applied energy 232 (2018) 54–68.
- [16] S. A. Pourmousavi, M. H. Nehrir, Real-time central demand response for primary frequency regulation in microgrids, IEEE Transactions on Smart Grid 3 (4) (2012) 1988–1996. doi:10.1109/TSG. 2012.2201964.
- [17] M. Vanouni, N. Lu, A reward allocation mechanism for thermostatically controlled loads participating in intra-hour ancillary services, IEEE Transactions on Smart Grid 9 (5) (2018) 4209–4219.
- [18] A. De Paola, V. Trovato, D. Angeli, G. Strbac, A mean field game approach for distributed control of thermostatic loads acting in simultaneous energy-frequency response markets, IEEE Transactions on Smart Grid (2019) 1–1doi:10.1109/TSG.2019.2895247.

- [19] W. Li, P. Du, N. Lu, Design of a new primary frequency control market for hosting frequency response reserve offers from both generators and loads, IEEE Transactions on Smart Grid 9 (5) (2018) 4883–4892. doi:10.1109/TSG.2017.2674518.
- [20] J. Wang, N. E. Redondo, F. D. Galiana, Demand-side reserve offers in joint energy/reserve electricity markets, IEEE Transactions on Power Systems 18 (4) (2003) 1300–1306. doi:10.1109/TPWRS. 2003.818593.
- [21] M. Parvania, M. Fotuhi-Firuzabad, Demand response scheduling by stochastic SCUC, IEEE Transactions on Smart Grid 1 (1) (2010) 89–98.
- [22] F. Partovi, M. Nikzad, B. Mozafari, A. M. Ranjbar, A stochastic security approach to energy and spinning reserve scheduling considering demand response program, Energy 36 (5) (2011) 3130 3137.
- [23] N. G. Paterakis, O. Erdin, A. G. Bakirtzis, J. P. S. Catalo, Qualification and quantification of reserves in power systems under high wind generation penetration considering demand response, IEEE Transactions on Sustainable Energy 6 (1) (2015) 88–103. doi:10.1109/TSTE.2014.2359688.
- [24] T. Wu, M. Rothleder, Z. Alaywan, A. D. Papalexopoulos, Pricing energy and ancillary services in integrated market systems by an optimal power flow, IEEE Transactions on Power Systems 19 (1) (2004) 339–347. doi:10.1109/TPWRS.2003.820701.
- [25] A. G. Vlachos, P. N. Biskas, Simultaneous clearing of energy and reserves in multi-area markets under mixed pricing rules, IEEE Transactions on Power Systems 26 (4) (2011) 2460–2471. doi:10.1109/ TPWRS.2011.2126025.
- [26] X. Gong, A. De Paola, D. Angeli, G. Strbac, A distributed price-based strategy for flexible demand coordination in multi-area systems, in: 2018 IEEE PES Innovative Smart Grid Technologies Conference Europe (ISGT-Europe), 2018, pp. 1–6.
- [27] F. Li, R. Bo, DCOPF-based LMP simulation: algorithm, comparison with acopf, and sensitivity, IEEE Transactions on Power Systems 22 (4) (2007) 1475–1485.
- [28] National Grid, Historical demand data (Nov. 2018).

  URL http://www2.nationalgrid.com/UK/Industry-information/
  Electricity-transmission-operational-data/Data-Explorer/
- [29] A. De Paola, X. Gong, D. Angeli, G. Strbac, Coordination of micro-storage devices in power grids: A multi-agent system approach for energy arbitrage, in: 2018 IEEE Conference on Control Technology and Applications (CCTA), 2018, pp. 871–878. doi:10.1109/CCTA.2018.8511352.